Sinusoidal phase-modulating laser diode interferometer capable of accelerated operations on four integrating buckets

Xuefeng Zhao, MEMBER SPIE
Takamasa Suzuki, MEMBER SPIE
Osami Sasaki, MEMBER SPIE
Niigata University
Faculty of Engineering
8050 Ikarashi 2
Niigata, 950-2181
Japan
E-mail: takamasa@eng.niigata-u.ac.jp

Abstract. We propose a sinusoidal phase-modulating laser diode interferometer that uses a charge-coupled device (CCD)-based additive operation on four integrating buckets. By shifting the injection-current bias of a laser diode to introduce additional phase shifts, a portion of the subtractive operations on the integrating buckets become additive operations, which are achieved in the CCD. This approach serves to reduce both data processing and measurement time. [DOI: 10.1117/1.1645252]

Subject terms: interferometers; laser diodes; integrating buckets; charge-coupled devices; sinusoidal phase modulation.

Paper 030346 received Jul. 17, 2003; revised manuscript received Sep. 8, 2003; accepted for publication Sep. 9, 2003.

1 Introduction

Several works have discussed the extraction of wavefront phases from interferograms by means of the integrating-bucket data collection technique.[1-6] Originally introduced in Ref. 1, the technique was used in our sinusoidal phase-modulating (SPM)[2] and SPM laser diode (LD)[3] interferometers. In SPM-LD interferometry, the interference signal's phase is varied by sinusoidally modulating the injection current of the LD. Collected during modulation, four interference-signal integrating buckets are used to determine the quadrature signal pair of the measurement phase.

As is common knowledge, a charge-coupled device (CCD) image sensor is a photodetector capable of integrating the intensity of the light on it, and generates a video signal based on that data. This CCD is suitable for collecting data in integrating-bucket method-based SPM interferometers. However, the evolution of CCD technology has brought with it pixel counts in the tens of millions. Along with the elevated pixel count, the volume of data being processed has greatly increased. To sustain such high data-processing speed, we found it necessary to employ an additive operation to integrating-bucket method-based SPM interferometry. When integrating-bucket data is being collected, by changing the LD's injection current, additional phase shifts in the interference signal are introduced, and a portion of the subtractive operations carried out on the integrating buckets becomes processes of addition. As the calculations are accomplished by the CCD, as opposed to the data processor, the burden of the latter can be reduced.

The first part of this work discusses the principle on which our design is based, as well as the methods used to implement it. We then provide a detailed description of measuring the diamond-turned aluminum disk with proposed interferometry. Systematic errors caused by faults in the phase shift are also analyzed.

2 Principle

2.1 *SPM Interferometry Using Integrating-Bucket Technique*

One of the useful features of LDs is their wavelength tunability.[3-5] When variable current $i_m(t)$ is injected into a LD, the intensity distribution of the interference pattern in a general two-beam interferometer can be expressed by

$$I(x,y,t)=I'(x,y)+I''(x,y)\cos[\phi(t)+\alpha(x,y)], \tag{1}$$

where

$$\phi(t)=\frac{4\pi l}{\lambda_0^2}\beta i_m(t) \tag{2}$$

is the phase change corresponding to the modulating current. $I'(x,y)$, $I''(x,y)$, $2l$, λ_0, β, and $\alpha(x,y)$ are background intensity, amplitude, optical path difference (OPD), the central wavelength of the LD, current modulation efficiency, and the phase to be measured, respectively. If the modulating current is a sinusoidal signal,

$$i_m(t)=m\cos(\omega_c t+\theta), \tag{3}$$

an SPM interferometer[7] can be constructed. The phase-modulated interference signal is given by

$$I(x,y,t)=I'(x,y)+I''(x,y)\cos[z\cos(\omega_c t+\theta)+\alpha(x,y)], \tag{4}$$

where

$$z=\frac{4\pi m\beta l}{\lambda_0^2} \tag{5}$$

represents modulation depth.

 0091-3286/2004/$15.00

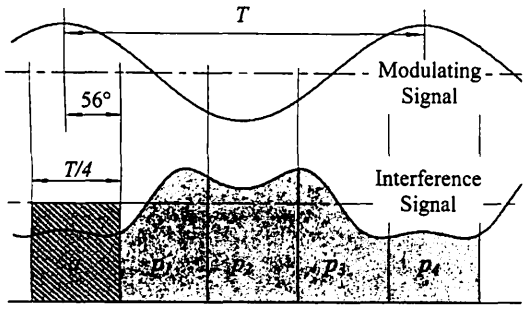

Fig. 1 Illustration of the integrating-bucket method used in the SPM interferometer.

Because the phase changes that occur in SPM interferometers are both continual and periodic, the integrating-bucket technique can be applied to extract phase $\alpha(x,y)$. Figure 1 illustrates the principle behind this method.[2] Within a given modulating period, the interference signal is integrated a total of four times, with the integrating time equaling a quarter of the modulating period. The integrated values are given by

$$p_i(x,y)=\int_{(i-1)T/4}^{iT/4}\{I'(x,y)+I''(x,y)\times\cos[z\cos(\omega_c t+\theta)+\alpha(x,y)]\}dt$$
$$=a(x,y)+b_i(x,y)\quad(i=1\sim4),\tag{6}$$

where a and b_i express integrated values of dc and ac components, respectively. We then derive the sine and cosine of wavefront phases

$$p_s(x,y)=(p_1-p_4)+(p_2-p_3)=A_s\sin\alpha(x,y),\tag{7}$$

and

$$p_c(x,y)=(p_1-p_4)-(p_2-p_3)=A_c\cos\alpha(x,y),\tag{8}$$

where A_s and A_c are functions of both modulation depth z and initial phase θ of the modulating current. They are given by

$$A_s=2I''(-8/\pi)\sum_{n=1}^{\infty}[J_{2n-1}(z)/(2n-1)](-1)^n\times\sin[(2n-1)\theta],\tag{9}$$

and

$$A_c=2I''(8/\pi)\sum_{n=1}^{\infty}[J_{2n}(z)/2n][1-(-1)^n]\sin(2n\theta),\tag{10}$$

where $J_n(z)$ is an n'th-order Bessel function. Setting $z=2.45$ and $\theta=56°$, $A_s=A_c$ is straightforward, with the noise-based measurement error being minimized.[2] The wavefront phase is then given by

$$\alpha(x,y)=\tan^{-1}\left[\frac{p_s(x,y)}{p_c(x,y)}\right]=\tan^{-1}\left(\frac{p_1+p_2-p_3-p_4}{p_1-p_2+p_3-p_4}\right).\tag{11}$$

2.2 *CCD-Based Additive Operation on Four Integrating Buckets*

In integrating-bucket method-based SPM-LD interferometry, as shown in Eqs. (7) and (8), at least one addition and three subtractions must be carried out to obtain the quadrature signal pair. Because Eqs. (7) and (8) are optimized algorithms, we have no other way of carrying out the operation, exclusive of the calculator, to reduce the number of operations. However, we can determine which CCDs are ideally suited if the equation forms are modified. The CCD also serves in the capacity of a bucket adder, because the additive operation on the adjacent integrating buckets is equivalent to successively integrating all buckets in the CCD. Hence, the method that uses CCD-based additive operations on four integrating buckets is proposed.

In Eq. (7) for example, expressing bucket data as the sum of a and b_i, we obtain

$$p_s=(a+b_1)+(a+b_2)-(a+b_3)-(a+b_4).\tag{12}$$

The bracketed terms are integrated in the CCD, and the remaining operations, in which subtractive operations exist, are calculated. By inserting $4a$ on both sides of Eq. (12), we obtain

$$P_s=p_s+4a=(a+b_1)+(a+b_2)+(a-b_3)+(a-b_4).\tag{13}$$

All operations between bracketed terms become additive operations, which are easily dealt with by the CCD. Subtractions carried out in the third and fourth terms are, in fact, additive operations of the dc components and the inverse of the ac components. In LD interferometers, inverting the sign of the ac component can be easily implemented by biasing the modulating current of the LD, in which a phase shift of π is introduced in the interference signal. The procedure is expressed by

$$p_i(x,y)=\int_{(i-1)T/4}^{iT/4}\left\{I'(x,y)+I''(x,y)\times\cos\left[z\cos(\omega_c t+\theta)+\frac{4\pi l}{\lambda_0^2}\beta\Delta i+\alpha(x,y)\right]\right\}dt$$
$$=\int_{(i-1)T/4}^{iT/4}\{I'(x,y)+I''(x,y)\times\cos[z\cos(\omega_c t+\theta)+\pi+\alpha(x,y)]\}dt$$
$$=a(x,y)-b_i(x,y)\quad(i=3,4).\tag{14}$$

Bias current Δi is determined by Eqs. (2) and (5) as

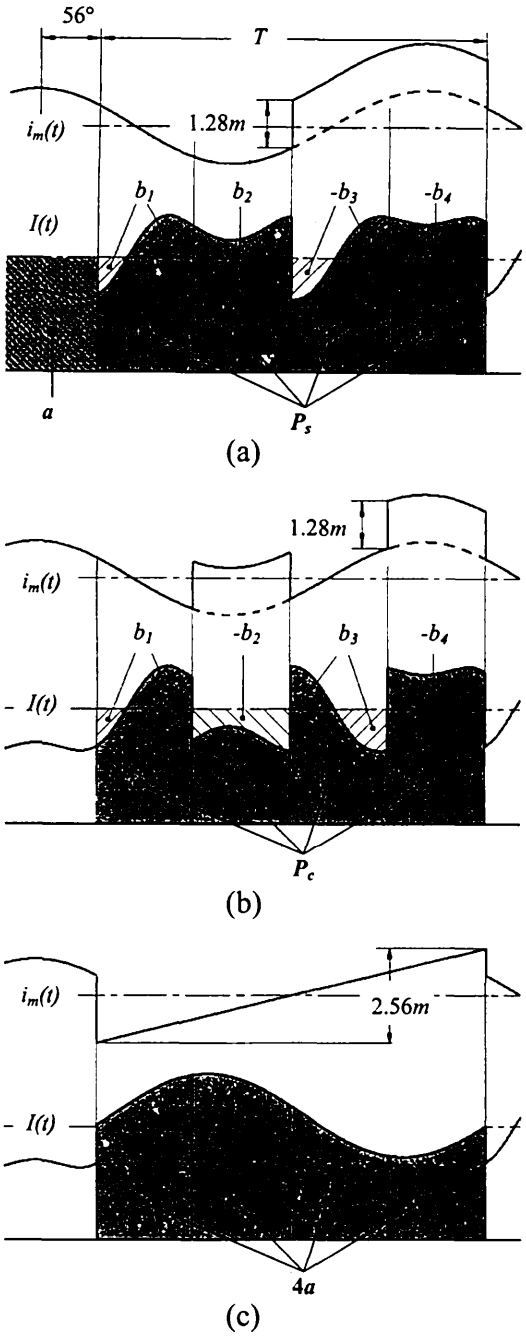

Fig. 2 Illustration of the CCD-based additive operation on four integrating buckets for obtaining (a) P_s, (b) P_c, and (c) 4a.

$$\Delta i=\frac{\lambda_0^2}{4\pi l\beta}\pi=\frac{m}{z}\pi. \tag{15}$$

Since we set the modulation depth z to equal 2.45,

$$\Delta i=\frac{\pi}{z}m\approx 1.28m. \tag{16}$$

We have proposed a high-speed modulating system that uses a common commercial CCD camera with high-speed shutter function.[8] The modulating frequency was not limited by the frame rate, and could be freely adjusted according to shutter speed. Through the use of this approach, as shown in Fig. 2(a), presetting the modulating period to the CCD's exposure time and biasing the modulating current by Δi during the second half-period, we obtain Eq. (13) in a single frame.

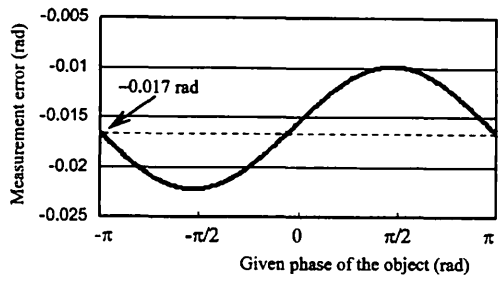

Fig. 3 Systematic error due to the phase-shifting error.

The extra term $4a$ in Eq. (13) is also obtained in the CCD, as

$$\int_0^T I(x,y,t)dt=\int_0^{2\pi}\{I'(x,y)+I''(x,y)\times\cos[\Delta\phi+\alpha(x,y)]\}d\phi=4a(x,y), \tag{17}$$

by linearly adjusting the interference signal's phase by 2π during modulating period T, as shown in Fig. 2(c), in which the change in injection current that produces the phase change of 2π is determined to $2.56m$.

Similarly, Fig. 2(b) demonstrates how, by inverting the signs of b_2 and b_4,

$$P_c=p_c+4a=(a+b_1)+(a-b_2)+(a+b_3)+(a-b_4) \tag{18}$$

is obtained in the CCD in the third frame.

The remaining processes are subtractions, $p_s=P_s-4a$ and $p_c=P_c-4a$, in the calculator. The amount of calculation is reduced by half in comparison with that in the conventional integrating-bucket method. In addition, with P_s, P_c, and $4a$ collected in three frames, data acquisition time is shortened as well.

2.3 *Error Analysis*

As described before, the sign inverse of the ac component in the interference signal is realized by shifting the interference signal's phase by π. Also, $4a$ is obtained by adjusting the interference signal's phase from 0 to 2π. Limitations in the experimental instrument prevent us from making accurate adjustments to the injection current of the LD to obtain desired phase shifts π and 2π. Such errors lead to the systematic error in our experiment. We evaluated the error based on computer simulations on the condition that the desired phase shift varies by 1%. The result is shown in Fig. 3 as the function of the object's phase. The measurement error combines bias with 360-deg periodicity due to the algorithm of the integrating-bucket method used in the SPM interferometer. The bias error induced by the phase-

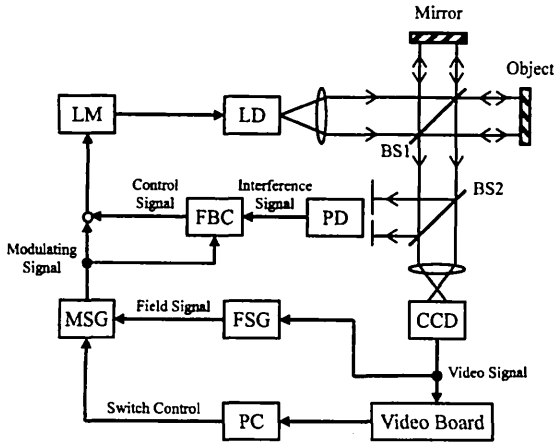

Fig. 4 Experimental setup. LD is the laser diode; LM is the laser diode modulator; BS is the beamsplitter; PD is the photodetector; FBC is the feedback controller; FSG is the field signal generator; and MSG is the modulating signal generator.

shifting error is -0.017 rad, which results in a measurement error of -0.93 nm at a LD wavelength of 685 nm. There is no great loss in accuracy.

Because the output wavelength of LD is determined by both the injection current and the junction temperature, it is necessary to consider the influence of the temperature fluctuation in most LD interferometers. In our case, however, such wavelength change can be automatically compensated by the feedback control, as described in the following section. The measurement error due to the junction temperature change can be neglected.

3 Experiments

Figure 4 details the experimental setup. The optical source of the Twyman-Green interferometer is the LD (Mitsubishi ML1412R), which features a central wavelength of 685 nm and 30 mW of output power. The interferometer consists of a reference mirror, an object, and a beamsplitter (BS1) with an OPD of 40 mm. Portions of the reference and the object beams pass through BS2 and interfere on the surface of the

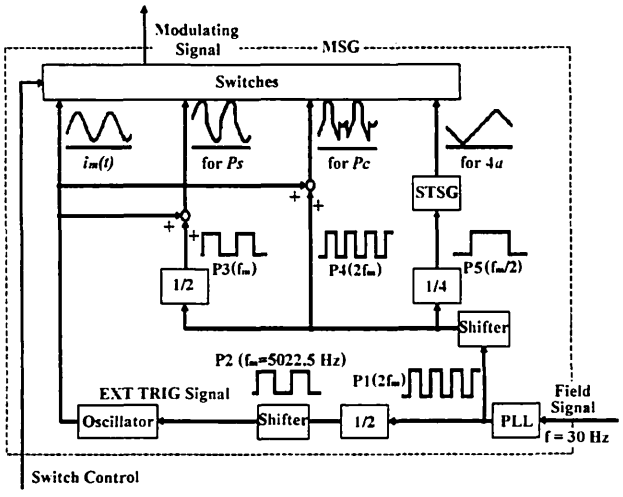

Fig. 5 Block diagram of the MSG. STSG is the sawtooth signal generator.

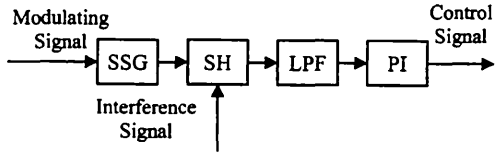

Fig. 6 Block diagram of the FBC. SSG is the sampling signal generator; SH is the sample-hold circuit; LPF is the low-pass filter; and PI is the proportional-integral controller.

CCD image sensor (Sony ICX058CL), whose pixel numbers are 768(H)×494(V) with a unit cell size of 6.35 μm(H)×7.40 μm(V). Its shutter speed is set to 1/5000 s. The modulating period and shutter speed are synchronized, which allows for a much higher modulating frequency and feedback-control speed. In this case, the actual integration time is 199 μs. We therefore adjusted the frequency of the sinusoidal modulating signal to $\omega_c/2\pi = 5022.5$ Hz. The CCD integrates the interferogram and produces the National Television System Committee (NTSC) video signal. Using a video capture board, we are able to acquire 320×240 pixel images.

Using a modulating signal generator (MSG), we generate the modulating signal from the field signal, which is first extracted from the video signal by a field signal generator (FSG). The block diagram of the MSG is shown in

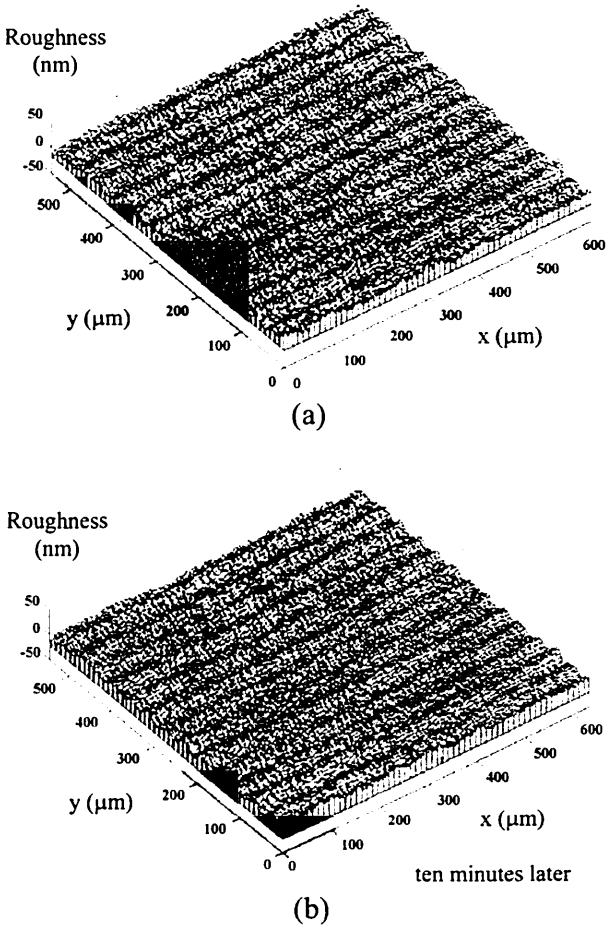

Fig. 7 3-D surface profiles of a diamond-turned aluminum disk.

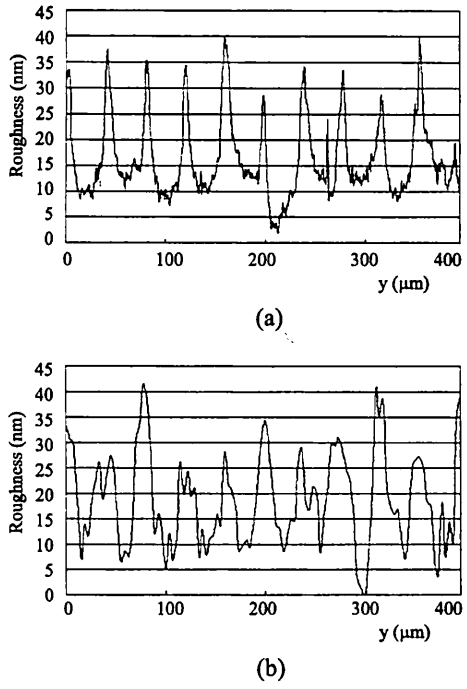

Fig. 8 2-D surface profiles of the diamond-turned aluminum disk measured with (a) a Talystep profilometer and (b) our system.

Fig. 5. Through a phase-locked loop (PLL), a pulse signal P1, whose frequency is twice that of $\omega_c/2\pi$, is generated. The sinusoidal modulating signal is the synthetic signal of pulse P2, whose frequency is half that of P1. To satisfy the conditions of $z=2.45$ and $\theta=56°$, the amplitude of the sinusoidal modulating signal is adjusted to $m=0.97mA$, and its initial phase is determined by adjusting the phase of P2. We then take P3, the frequency of which is only half as high as P1, and P4, whose frequency equals that of P1, knowing that their pulse heights are both $1.28m$. These pulses are mixed with the sinusoidal signal so that they generate the modulating signal necessary for obtaining P_s and P_c. Then by employing a 1/4 frequency divider and a sawtooth signal generator (STSG), we create a modulating signal with a slope of $2.56m/T$ from P1, thereby obtaining $4a$. With the selection of these modulating signals being controlled by the computer, we obtain the modulating signals shown in Fig. 2.

After being reflected by BS2, the reference and the object beams interfere on the surface of the photodetector (PD). The interference signal detected by PD is injected into the feedback controller (FBC). Figure 6 shows the block diagram of the FBC. In the FBC, the sampling pulse synchronized with the modulating signal is generated in the sampling signal generator (SSG) and samples the interference signal through the sample-hold circuit (SH). Then the output signal is smoothed by a low-pass filter (LPF), whose cut-off frequency is 1 kHz. After passing a proportional-integral (PI) controller, the control signal is finally obtained. By using the phase-locked technique,[9] we effectively eliminate the external disturbance and the undesirable LD's wavelength change.

We measured the surface profile of a diamond-turned aluminum disk with the present experiment setup. Figure 7 shows the measurement results. The ditch shape cut by the diamond bite is clearly discernible. The same position was measured several times at intervals of ten minutes. We obtained a repeatability of 5.93-nm rms. Two 2-D profiles measured with the Taly-step profilometer and the interferometer we propose are given in Figs. 8(a) and 8(b), respectively. Although the measured positions are different, the roughness and the cutting pitch are in good agreement.

4 Conclusion

We propose a sinusoidal phase-modulating laser diode interferometer that uses an accelerated integrating-bucket method, and demonstrate some 3-D measurements. Through the use of the additive operation on four CCD buckets, we are able to both lighten the computer's burden, which helps maintain processing speed when huge data volume is required in the measurement, and reduce measurement time.

References

1. J. C. Wyant, "Use of an ac heterodyne lateral shear interferometer with real-time wavefront correction system," *Appl. Opt.* **14**, 2622–2626 (1975).
2. O. Sasaki, H. Okazaki, and M. Sakai, "Sinusoidal phase modulating interferometer using the integrating-bucket method," *Appl. Opt.* **26**, 1089–1093 (1987).
3. T. Suzuki, O. Sasaki, S. Takayama, and T. Maruyama, "Real-time displacement measurement using synchronous detection in a sinusoidal phase modulating interferometer," *Opt. Eng.* **32**, 1033–1037 (1993).
4. K. Tatsuno and Y. Tsunoda, "Diode laser direct modulation heterodyne interferometer," *Appl. Opt.* **26**, 37–40 (1987).
5. J. Chen, Y. Ishii, and K. Murata, "Heterodyne interferometry with a frequency-modulated laser diode," *Appl. Opt.* **27**, 124–128 (1988).
6. A. Dubois, "Phase-map measurements by interferometry with sinusoidal phase modulation and four integrating buckets," *J. Opt. Soc. Am. A* **18**, 1972–1979 (2001).
7. O. Sasaki and H. Okazaki, "Sinusoidal phase modulating interferometry for surface profile measurement," *Appl. Opt.* **25**, 3137–3140 (1986).
8. T. Suzuki, T. Maki, X. Zhao, and O. Sasaki, "Disturbance-free high-speed sinusoidal phase-modulating laser diode interferometer," *Appl. Opt.* **41**, 1949–1953 (2002).
9. T. Suzuki, O. Sasaki, and T. Maruyama, "Phase locked laser diode interferometry for surface profile measurement," *Appl. Opt.* **28**, 4407–4410 (1989).

Xuefeng Zhao received his BE degree from the Beijing Institute of Technology in 1992, and his ME degree from Niigata University in 2002, all in electrical engineering. He is currently pursuing his PhD degree in electrical engineering at Niigata University. Since 1998, he has researched optical metrology and optical information processing at Niigata University.

Takamasa Suzuki received his BE degree in electrical engineering from Niigata University in 1982, his ME degree from Tohoku University in 1984, and his PhD degree in electrical engineering from Tokyo Institute of Technology in 1994. He is an associate professor of electrical and electronic engineering at Niigata University. His research interests include optical metrology, optical information processing, and phase-conjugate optics.

Osami Sasaki received his BE and ME degrees in electrical engineering from Niigata University in 1972 and 1974, respectively, and his PhD degree in electrical engineering from Tokyo Institute of Technology in 1981. He is a professor of electrical and electronic engineering at Niigata University. Since 1974, he has worked in the field of optical measuring systems and optical information processing.